J Membrane Biol (2007) 216:1–16
DOI 10.1007/s00232-007-9019-y

TOPICAL REVIEW

The Lens Circulation

Richard T. Mathias · Joerg Kistler · Paul Donaldson

Received: 23 January 2007 / Accepted: 4 April 2007 / Published online: 14 June 2007

Abstract The lens is the largest organ in the body that lacks a vasculature. The reason is simple: blood vessels scatter and absorb light while the physiological role of the lens is to be transparent so it can assist the cornea in focusing light on the retina. We hypothesize this lack of blood supply has led the lens to evolve an internal circulation of ions that is coupled to fluid movement, thus creating an internal micro-circulatory system, which makes up for the lack of vasculature. This review covers the membrane transport systems that are believed to generate and direct this internal circulatory system.

Keywords Ion transport · Fluid transport · Volume regulation · Glucose transport · Amino acid transport

Introduction

The lens circulation was previously reviewed by Mathias, Rae & Baldo (1997) and Donaldson, Kistler & Mathias, 2001), so we will provide a less detailed summary of the older data and a more intuitive description of how these data and more recent studies link to the lens circulation. The review begins with the basic biophysical properties of the lens and how they affect the circulation and then reviews the molecular identification and localization of a wide variety of channels and transporters that underpin fluid movement. Lastly, we review functional experiments that provide direct evidence of how this unique circulation system enables the fiber cells buried deeply in the lens core to take up nutrients and antioxidants for the maintenance of tissue transparency.

R. T. Mathias (✉)
Department of Physiology and Biophysics, State University of New York at Stony Brook, , Stony Brook, NY, New York 11794-8661
e-mail: richard.mathias@sunysb.edu

J. Kistler
School of Biological Sciences, University of Auckland, 3 Symonds Street, Private Bag 92019, Auckland, New Zealand

P. Donaldson
Department of Physiology, University of Auckland, 85 Park Road, Auckland, New Zealand

Structure and Development

The cellular architecture of the adult lens is sketched in Figure 1 (Kuszak & Rae, 1982; Zampighi, Eskandari & Kreman, 2000). This structure is in place by birth and continues to grow throughout the lifetime of the animal, though growth slows considerably in the adult (*reviewed in* Maisel et al., 1981). The anterior surface of the lens is a single layer of epithelial cells. At the equator, these cells begin to elongate and differentiate into the fiber cells that make up the bulk of the lens. As the fiber cells elongate and become completely internalized, their ends are joined by collagen at sutures that run from the lens center to anterior and posterior poles (*reviewed in* Kuszak et al., 1984). New shells of fiber cells are continually laid on top of the older cells, so depth within the lens relates to cell age and stage of development.

Localization of Cellular Properties

Our current state of understanding of the functional and morphological variations within the lens is probably still too simple, but the localizations described below are the minimum that need to be addressed. The morphology of

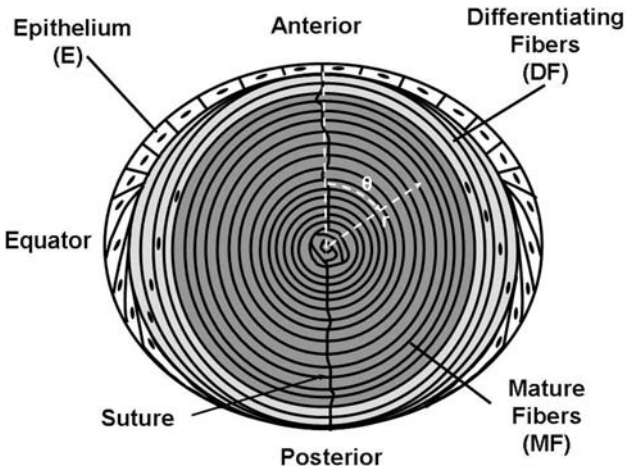

Fig. 1 A sketch of the lens structure. Membrane transport differs in the radial zones identified as epithelium, differentiating fibers and mature fibers. Moreover, within each radial zone there are differences in angular locations between the equator and poles. A spherical coordinate system is defined to identify location in terms of distance from the lens center, r (cm), and angular distance from the anterior pole, θ (radians)

the epithelial cells in the mammalian lens changes from flat at the anterior, where the cells are inert, to cuboidal at halfway between pole and equator in the zone of cell division to elongated at the equator, where epithelial-fiber cell differentiation is initiated (Menko, 2002). Although Figure 1 is not drawn to scale, it illustrates these changes in epithelial cell shape. Membrane transport also varies in the epithelium as one looks from the equator to the anterior pole (Gao et al., 2000; Candia & Zamudio, 2002; Tamiya et al., 2003).

The differentiating fiber cells (DF in Fig. 1) contain intracellular organelles and are able to perform protein synthesis. There are a number of DF-specific membrane transport systems (Donaldson et al., 2004). Moreover, within the DF there are also angular variations in transport as the gap junction coupling conductance varies from equator to both poles (Baldo & Mathias, 1992).

At about 15% of the distance into the lens, the fiber cells lose their organelles (Bassnett, 2002), many membrane transport proteins are modified through cleavage, gap junction plaques are reorganized and several membrane proteins are inserted into the plasma membrane from a pool of endosomal vesicles (Ball et al., 2004; Donaldson et al., 2004; Jacobs et al., 2004; Yin, Gu & Jiang, 2001a,b; Lin et al., 1997). The loss of organelles minimizes light scattering; however, it means the inner core of organelle free mature fibers (MF in Fig. 1) must survive the lifetime of the animal without *de novo* synthesis of proteins.

Studies of cellular transport properties in the lens require the specification of spatial location, which we will define using spherical coordinates. The radial coordinate, r (cm), gives the distance from the lens center ($r = 0$) to the surface ($r = a$). The DF-to-MF transition is sufficiently abrupt that it can be defined as $r = b$ ($b \approx 0.85a$). The angular coordinate, θ (degrees), gives the distance from the anterior pole ($\theta = 0^o$) to the equator ($\theta = 90^o$) to the posterior pole ($\theta = 180^o$). Insofar as we are aware, the lens is structurally and functionally symmetric about a line passing through the anterior and posterior poles (sutures in Fig. 1); hence, two coordinates are sufficient to determine functional and structural locations.

Anisotropies, Morphometrics and Transport

The fiber cell structure of the lens creates significant differences in the θ *vs.* r direction for the diffusion of solutes and flow of ionic current. Figure 2a illustrates the structure and packing of the fiber cells. In cross section, each cell is a flattened hexagon whose dimensions are approximately 3 x 9 μm. Thus, intracellular current flow in the r direction must cross a gap junction every 3 μm (Fig. 2b). Though the cells are exceptionally well coupled, gap junctions must be traversed so frequently that they are rate-limiting for intracellular diffusion or ionic current flow. The effective intracellular radial resistivity (R_{ir}, Ωcm) is defined experimentally by injecting a current and measuring the induced intracellular voltage gradient in the radial direction. By Ohm's law in a continuum,

$$i_r = -\frac{1}{R_{ir}}\frac{\partial \psi_i}{\partial r} \tag{1}$$

The radial resistance is primarily due to gap junctions, which occur at discrete locations, so the intracellular compartment is not a continuum. However, because the radial distance between gap junctions (3 μm) is short in comparison to the length constant for radial current flow (600 μm; Baldo & Mathias, 1992), the intracellular compartment can be treated as a continuum with an effective radial resistivity:

$$R_{ir} \approx R_j / 3x10^{-4} \tag{2}$$

where R_j (Ωcm^2) is the gap junction coupling resistance of a unit area of cell-to-cell contact and 3 x 10^{-4} cm is the radial distance between gap junctions.

In contrast, in the θ direction, the axes of fiber cells extend from anterior to posterior sutures (Fig. 1); hence, intracellular current flow or diffusion does not traverse any gap junctions and the resistivity is that of cytoplasm. In a mammalian lens, the average effective resistivity in the r direction of the DF is about 3,000 Ωcm and in the MF about 6,000 Ωcm (*reviewed in* Mathias et al., 1997), whereas the resistivity of cytoplasm ρ_i (Ωcm, $\rho_i = R_{i\theta}$) is

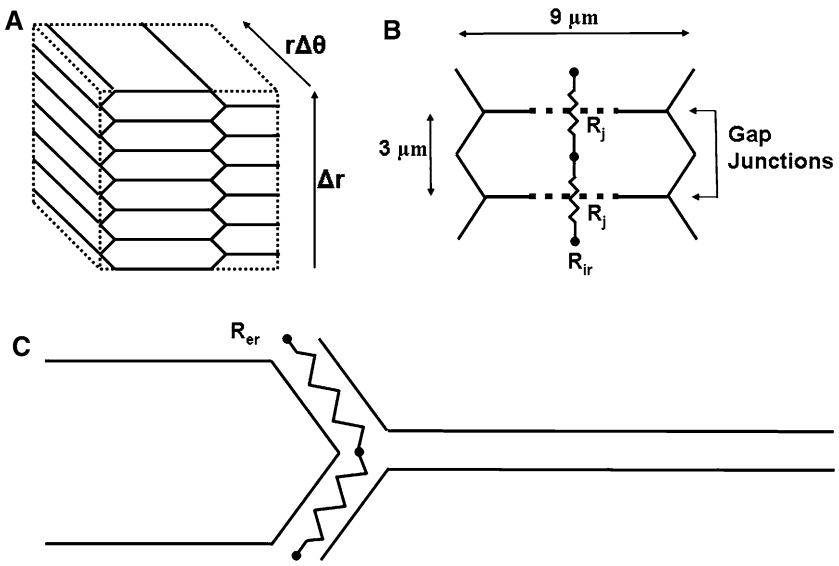

Fig. 2 Packing of lens fiber cells and its effect on ion fluxes. Within the lens, ion fluxes can exist in either the intracellular or extracellular compartments. (**a**) A cuboid of lens tissue. For analysis of ionic current flow, such a cuboid is assumed to be small in comparison to the length constant for current flow but large enough to contain a representative segment of fiber cells and extracellular space. (**b**) Gap junctions connecting fiber cells in the radial direction. The effective intracellular radial resistivity, R_{ir} (Ωcm), is determined by the gap junction resistance, R_j (Ωcm^2), divided by the radial distance between gap junctions (about 3 µm). (**c**) Path for radial extracellular current flow. About two-thirds of the extracellular volume does not contribute to the effective extracellular radial resistivity, R_{er} (Ωcm), and the path that does is not a straight line

on the order of 150 Ωcm. Hence, voltage gradients in the θ direction will be 20–40 times smaller than those in the r direction. Mathias & Rae (1985) reported there were intracellular radial voltage gradients on the order of 10 m*V*/mm in the frog lens, but no measurable gradients in the θ direction have been reported by any investigator studying the lens resting voltage (*reviewed in* Mathias et al., 1997). Hence, when Robinson & Patterson (1982) first reported significant θ dependence for the lens circulating currents (reviewed in the next section), there was widespread surprise and reservation. In retrospect, consideration of the anisotropic structure of the lens should have made their finding less surprising, but hindsight is always clearer.

Current also circulates through the lens along the narrow tortuous extracellular spaces between cells. When deriving equations to describe current flow in a syncytium like the lens, it is convenient to analyze a cuboid of tissue (Fig. 2a) that contains a number of cells as well as extracellular space yet is small relative to the length constants for current flow (Mathias, Rae & Eisenberg, 1979; Peskoff, 1979). Thus, the coordinate location r,θ defines the position of a small cuboid of tissue, and intracellular and extracellular current flows share the same location. About 99% of the volume of the cuboid is intracellular space, so we assume the intracellular volume fraction $V_i/V_T \approx 1.0$ and ignore it. The effective extracellular radial resistivity within the cuboid depends on the cross section and radial length of cleft, which is assumed to depend on the volume fraction V_e/V_T times a tortuosity factor, τ_r. Thus, if ρ_e (Ωcm) is the resistivity of extracellular saline, then the effective extracellular resistivity in the radial direction is given by

$$R_{er} = \rho_e / \left(\tau_r \frac{V_e}{V_T} \right) \tag{3}$$

Mathias (1983) showed that the tortuosity factor depends on a branching factor times a length factor. If one considers the sketch in Figure 2c for radial extracellular current flow, about two-thirds of the clefts branch in a direction perpendicular to radial flow; thus, the first component of the tortuosity factor is 1/3 to account for the fraction of the extracellular volume that conducts radial flow. The second component, which accounts for the extra length of flow, is about $1/\sqrt{2}$, assuming the ends of the hexagons are near to right triangles. Thus, the tortuosity factor is $\tau_r = 1/6$, or $\tau_r \approx 0.17$. The width of the clefts is 30–40 nm, which implies a volume fraction $V_e/V_T \approx 0.015$. Thus, $R_{er} \approx 400\rho_e$. Mathias et al. (1997) review data from impedance experiments on intact lenses; the experimental value of R_{er} in mammalian lenses is about 26,000 Ωcm, which is consistent with the above-described morphology of the extracellular spaces and a resistivity $\rho_e = 65$ Ωcm. The effective extracellular resistivity in the θ direction has not been measured; however, there is no effect of tortuosity

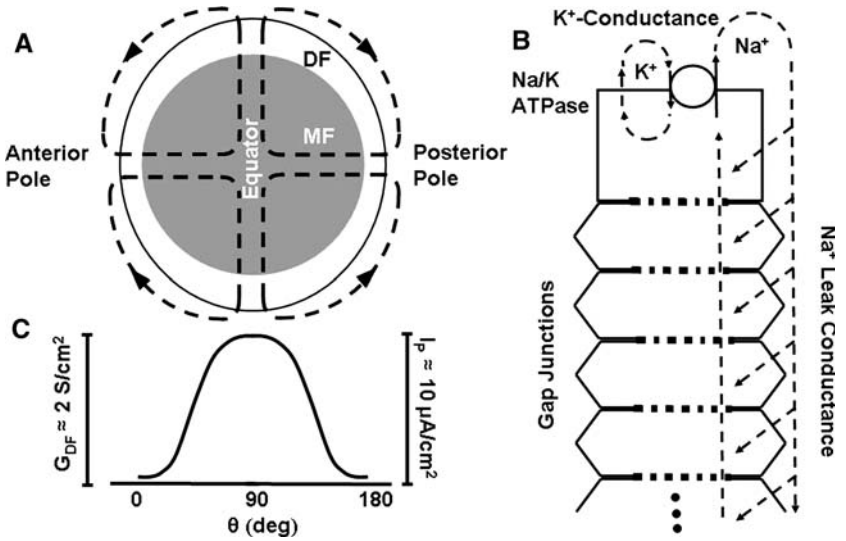

Fig. 3 The lens circulation. (**a**) Pattern of current flow. Current enters the lens at both poles and exits at the equator. (**b**) Factors responsible for generating current flow. The transmembrane sodium gradient, which is generated by the Na/K pumps, pulls sodium across fiber cell membranes from the extracellular to the intracellular space. Thus, inward radial current is extracellular, whereas outward radial current is intracellular. (**c**) Factors responsible for directing the pattern of current flow. DF gap junctional coupling conductance, G_{DF} (S/cm^2), is highest at the equator and directs the outward radial intracellular current to the equatorial surface. Na/K pump current density, I_P (μA/cm^2), is highest at the equatorial surface, where the pumps are concentrated to transport the circulating flux of sodium out of the lens

in this direction, so the value should be $R_{e\theta} = \rho_e/(V_e/V_T)$, which would be around 4,300 Ωcm.

An important point of this analysis is that by defining an experimentally measurable effective extracellular resistivity we have transformed the current density within a cleft to an average in a unit volume of tissue. Thus, the radial current density within the clefts is actually about 400 times greater than that calculated using the effective resistivity. In other words, the extracellular equation for Ohm's law in the syncytium:

$$i_{er} = -\frac{1}{R_{er}}\frac{\partial \psi_e}{\partial r} \tag{4}$$

where ψ_e is the voltage in the extracellular clefts, is valid for the current density entering a cuboid of tissue. Since the clefts are a small fraction of the cuboid, the actual current density within a cleft is much larger than that calculated using equation 4. This becomes particularly important when we consider water flow, which is rather slow when calculated for a unit volume of lens tissue but becomes respectably fast when one considers the actual velocity within a cleft.

In the lens, the epithelium carries out essentially all of the active transport (Paterson & Delamere, 2004); however, there is a large discrepancy between the amount of epithelial cell membrane compared to that of fiber cells. The total area of fiber cell membrane is given by the volume ($4\pi a^3/3$) times the average surface of membrane in a unit volume of tissue ($S_m/V_T \approx 6{,}000$ cm^{-1}; Mathias et al., 1997). If the epithelial cells were simple cubes with six smooth sides, then the surface area of epithelial cell membrane would be $6 \times 2\pi a^2$. Thus,

$$\frac{\textit{fiber membrane}}{\textit{epithelial membrane}} \approx \frac{a}{9}\frac{S_m}{V_T} \tag{5}$$

For a small mouse lens whose radius $a = 0.05$ cm, the epithelium represents about 3% of the total membrane, whereas for a rabbit lens of radius $a = 0.5$ cm, the epithelium is only 0.3% of the total fiber cell membrane. The relatively large area of fiber cell membrane means that even a small current in each individual fiber cell becomes a large total current at the surface of the lens, and this is the basis of the lens circulation.

The Lens Circulation

Figure 3a illustrates the net current entering the lens at each pole and exiting at the equator. The lines of current flow are not intended to be exact, and they are almost certainly too simple within the lens, owing to the anisotropies just described. However, they illustrate continuity of current flow and equality between what enters and exits. This pattern of current was first detected by Robinson & Patterson (1982) using a vibrating probe to measure extracellular current around the rat lens. It has subsequently

been measured in other species by other investigators, using both the vibrating probe and an Ussing-like chamber to isolate sections of the lens surface (Parmelee, 1986; Candia & Zamudio, 2002).

Mechanisms Generating the Lens Circulation

Na^+ currents

For the moment, the pattern of flow will be ignored and we will focus on the factors that generate the circulation. Our hypothesis is that it is a circulation of Na^+ (Fig. 3b). This hypothesis is based on the following observations. The Na/K pumps are located in the surface epithelial cells (*reviewed in* Delamere & Tamiya, 2004; Mathias et al., 1997). These pumps generate a typical low intracellular Na^+ concentration and a high intracellular K^+ concentration (Paterson, 1972; Paterson et al., 1974) in all cells of the lens. The lens resting voltage is typically –70 m*V*; hence, there is a large electrochemical gradient for Na^+ influx into all cells of the lens. All lens cells have a small Na^+ permeability (Mathias et al., 1985), but because of the large number of fiber cells, this small permeability leads to a significant total influx of Na^+. All fiber cells are interconnected by a network of low-resistance gap junctions (*reviewed in* DeRosa et al., 2005). Thus, when Na^+ enters fiber cells from the extracellular spaces within the lens, it flows from fiber cell to fiber cell through gap junctions to the surface epithelial cells, where it is transported out of the lens by the Na/K pumps. In this model of circulating Na^+ current, extracellular current flows inward from the lens surface toward the center, whereas intracellular current flows outward from the center toward the surface.

This model suggests there are three major components of the lens circulation: epithelial Na/K pumps, fiber cell gap junctions and fiber cell Na^+ channels. Of these, the molecular identity of only the Na^+ channels remains unknown. One possibility is that Na^+ enters the fiber cells through gap junction hemichannels. Both of the fiber cell connexins, Cx46 and Cx50, can form hemichannels that, if open, would cause a nonselective leak channel (Ebihara, 2003a,b). Under normal physiological conditions, hemichannels have a very low open probability, which is consistent with the fiber cell membrane Na^+ conductance being very low (~1 $\mu S/cm^2$). To put this into context, the cell-to-cell conductance is about 1 S/cm^2, and assuming each channel has a conductance on the order of 200 pS, this would require 50 open channels/μm^2. If we assume an open hemichannel has twice this conductance, the membrane conductance would require only 1 open channel/40,000 μm^2. Obviously, such a rare event is difficult to study; hence, there is no direct evidence on the molecular identity of the channel.

K^+ currents

The other major cation, K^+, appears to be handled quite differently. Mathias et al. (1985) suggested the fiber cells lack the high K^+ conductance present in most cells, and this conclusion has subsequently been supported by more direct patch-clamp studies of isolated fiber cells (Webb, 2006). The lens epithelial cells, however, appear to have a more typical high K^+ conductance (Cooper et al., 1990; Cooper, Watsky & Rae, 1992; Miller, Zampighi & Hall, 1992; Rae & Rae, 1992). Thus, the K^+ that is transported into lens cells by the Na/K pumps mostly leaks out of the same cells (Fig. 3b), contributing little to the net circulation (Mathias et al., 1985; Candia & Zamudio, 2002). If the fiber cells did indeed have a significant K^+ conductance, the resulting K^+ current would flow in the opposite direction to the Na^+ current, thus reducing the net current; so the surface localization of K^+ channels is a key feature of the circulation.

The molecular identity of the lens K^+ channels is an interesting story that illustrates a general issue in using animal models for human diseases. Lenses from all species studied express more than one type of K^+ channel, and each species expresses different types (*early studies reviewed in* Mathias et al., 1997; Shepard & Rae, 1998,1999; Rae & Shepard, 1998–c, 2000a,b). One view would be that there is no appropriate animal model for the human lens. However, from a different perspective, all lenses express their K^+ channels exclusively in the epithelium and have a circulation. Thus, from the perspective of the forest, all lenses become the same, but if one looks at the trees, differences appear. The reason for this diversity is not known, but one simple factor could be size. Total Na^+ conductance increases with the volume of the lens, whereas total K^+ conductance depends on the surface area of the epithelium. As a consequence, as lenses from large mammals grow, the volume-located Na^+ conductance increases more rapidly than the surface-located K^+ conductance and they tend to depolarize. Delayed rectifier-type K^+ channels would act as a brake on this depolarization, and they are indeed found in the larger lenses from humans, cows and pigs (Cooper et al., 1990; Rae, 1994; Rae & Rae, 1992), whereas lenses from smaller animals tend to express inward rectifier-type K^+ channels (Cooper, Rae & Dewey, 1991).

Cl^- currents

The major anion, Cl^-, also acquires a unique steady state, which has a significant role in lens cell volume regulation but not in the lens circulation under basal conditions. The fiber cell Cl^- conductance appears to have a value similar to that of the Na^+ conductance (Mathias et al., 1985), both being on the order of 1 $\mu S/cm^2$ in a mammalian lens

(Table 1 of Mathias et al., 1997). The transmembrane Cl^- gradient, however, is close to electrochemical equilibrium, whereas the Na^+ gradient is far from equilibrium; hence, Cl^- currents are relatively small and have only a small modulatory effect on the circulation. The lens handling of Cl^- is therefore reviewed later (*see* Lens Cell Volume Regulation).

Summary

The ultimate source of energy for the lens circulation is Na/K-ATPase, which generates the transmembrane electrochemical gradient for Na^+. The circulation occurs because the site of leak of Na^+ down its gradient into the intracellular compartment (the fiber cells) is spatially distinct from the site of active transport of Na^+ out of the intracellular compartment (the epithelium). These ideas are summarized in Figure 3b. The transmembrane fluxes of other ions have relatively minor effects on the net current generated by the transmembrane fluxes of Na^+.

Factors Directing the Lens Circulation

Gap junctions

Mammalian lens gap junctions are made from three different connexins: Cx43, Cx50 and Cx46 (*reviewed in* DeRosa et al., 2005). The epithelial cells synthesize Cx43 and Cx50, but at the E-DF transition, Cx43 expression is lost. In the DF, Cx46 and Cx50 are expressed and both appear to make functional channels, but at the DF-MF transition, functional Cx50 channels appear to be lost (Gong et al., 1998; Baldo et al., 2001; Martinez-Wittinghan et al., 2004), although the Cx50 protein remains present in a truncated form (Kistler & Bullivant, 1987; Kistler, Kirkland & Bullivant, 1985).

Baldo & Mathias (1992) performed impedance studies to determine membrane conductance and gap junction coupling conductance at different θ locations around the intact rat lens. There was no correlation between membrane conductance and the pattern of the circulation; however, the gap junction coupling conductance of DF (G_{DF} S/cm^2) was found to be highest at the equator and lowest at either pole (Fig. 3c). In contrast, they could not detect any significant θ dependence for the coupling conductance of the MF. For simplicity, we assume the transition from uniform coupling in the MF to θ-dependent coupling in the DF occurs in a step-like manner at the DF-MF transition. When a current is injected into a central fiber cell, the experimental measurement of the θ dependence of the induced voltage is greatly smoothed because the highest current density occurs where the coupling conductance is highest. Furthermore, the anisotropic structure of the fibers tends to even out the θ dependence of the induced voltage. For these reasons, the estimate of G_{DF} is subject to considerable uncertainty. We assume G_{DF} is a smooth function of θ and it varies from its minimum value at either pole (G_{min}) to its maximum value at the equator (G_{max}), as shown in Figure 3c. At $\theta = 45^o$ or 135^o, the current density and the coupling conductance should be close to the angular average. Since the estimated value of G_{DF} at these locations is about 1 S/cm^2, the maximum should be about twice that and the minimum can be no less than zero. Figure 3c and equation 6 are based on these assumptions.

$$G_{DF} = G_{min} + (G_{max} - G_{min}) \sin^2 \theta \quad (6)$$

This representation of G_{DF} is almost certainly too simple, but it provides a picture that one can use to think about the properties of coupling in DF of the lens.

Mathias et al. (1997) suggested the angular variation in conductance might be due to higher expression levels of connexins in the newly developing equatorial fiber cells, but this is probably not the mechanism as immunostaining of lens connexins does not show a dramatic loss of signal at the poles (Gruijters et al., 1987; Berthoud, Cook & Beyer, 1994; Dahm et al., 1999). Le & Musil (2001) provided an alternative explanation: they showed that fibroblast growth factor (FGF) upregulated gap junction coupling in primary cultures of chick lens epithelial cells undergoing epithelial-to-fiber differentiation. An FGF-like factor was indeed present in the vitreous, and FGF-signaling occurred in the equatorial cells of the intact lens. They suggested an FGF-mediated increase in the number of open gap junction channels in the equatorial DF, whereas the total number of channels was more uniform around the DF. This fits more reasonably with the rather abrupt switch from θ-dependent conductance in the DF to θ-independent coupling in the MF. One can easily conceive of posttranslational modifications or a reduction in FGF signaling at this transition generating a more uniform open probability. It is much more difficult to conceive of channels being absent from the polar regions of DF but suddenly appearing in the polar regions of MF.

Na/K pumps

Na/K-ATPase comprises an α- and a β-subunit (*reviewed in* Gick et al., 1993; Sweadner, 1989) and sometimes a γ-subunit referred to as ''phospholemman'' (Geering, 2006). The α-subunit uses the energy of one ATP to transport three Na^+ out of a cell and two K^+ into the cell, whereas the β- and γ-subunits appear to have modulatory roles. The α1, α2 and α3 isoforms are widely expressed throughout the body as well as in the eye. The isoform distribution in the lens depends on the species.

Candia & Zamudio (2002) used an Ussing-like chamber to isolate different regions of the rabbit lens surface and measure the local current densities. By local application of ouabain, a specific inhibitor of Na/K-ATPase, they were able to map the surface distribution of Na/K pump current (I_P, μA/cm^2). They concluded that I_p was too small to detect at either pole but reached a maximum of 10 μA/cm^2 at the equator (sketched in Fig. 3c and given by equation 6 with substitution of I_P for G_{DF}, of I_{max} for G_{max} and of I_{min} for G_{min}). This equatorial concentration of I_P was consistent with whole-cell patch-clamp studies of isolated epithelial cells from the equatorial and polar regions of the frog lens (Gao et al., 2000) and porcine lens (Tamiya et al., 2003). As sketched in Figure 3b, most of the K^+ transported into the epithelial cells by the Na/K pumps is essentially balanced by an equal and opposite leak of K^+ out of these same cells; hence, the net current leaving the lens at the equator will be carried mostly by Na^+. Since the Na/K pump has a stoichiometry of 3Na:2K, its outward Na^+ current will be $3I_P$, or about 30 μA/cm^2, which is near the value of the lens circulating current detected at the equator using either the vibrating probe or an Ussing-like chamber (Robinson & Patterson, 1982; Parmelee, 1986; Candia & Zamudio, 2002).

The isoform expression of Na/K-ATPase is species-specific (Garner & Horowitz, 1994; Gao et al., 2000; Paterson & Delamere, 2004), whereas its localization to the equatorial epithelium has been found in all species examined (specifically in rabbit, frog and pig) and is likely to be a ubiquitous property. As was the case with lens K^+ channels, if one views the Na/K pumps as a component of the entire lens circulation system, then it is consistent in all species studied; but if one looks closer, species-related differences appear. The reasons for this heterogeneity between species are not known, but one possibility is that different isoforms are separately regulated, as is known to occur in the heart (*reviewed in* Mathias, Cohen, Gao & wang, 2000).

Summary

Na^+ that enters the central fiber cells initially flows back toward the surface in essentially a spherically symmetric pattern, but as it approaches the DF, it is directed to the equator by the relatively high gap junction coupling conductance of the equatorial DF. When this intracellular flow of Na^+ reaches the equatorial epithelial cells, it is transported out of the lens by the relatively high concentration of Na/K pumps in this population of cells. Thus, the coupling conductance of the DF and the Na/K pump distribution in the epithelium appear to be the key features directing the current to flow in its dramatic circulating pattern.

The Physiological Role of the Lens Circulation

Circulating currents have been found in lenses from every species studied. One therefore assumes that such a system must be a central component of homeostasis for the normal lens. Our working hypothesis is the transport of Na^+ is linked through local osmosis to the movement of fluid (Mathias, 1985; Mathias et al., 1997; Mathias & Wang, 2005), which circulates in the same pattern as Na^+ (Fig. 4). As fluid moves into the lens along the extracellular spaces, it carries metabolites such as glucose, antioxidants such as ascorbate and amino acids to the deeper lying fiber cells, providing them with the factors needed for homeostasis. The circulating pattern of flow ensures maximum stirring of the fluid entering the extracellular spaces so that solution depleted of the above factors will not be recirculated.

Lens fluid transport

The above hypothesis is based on model calculations (Mathias, 1985) around standard thermodynamics of sol-

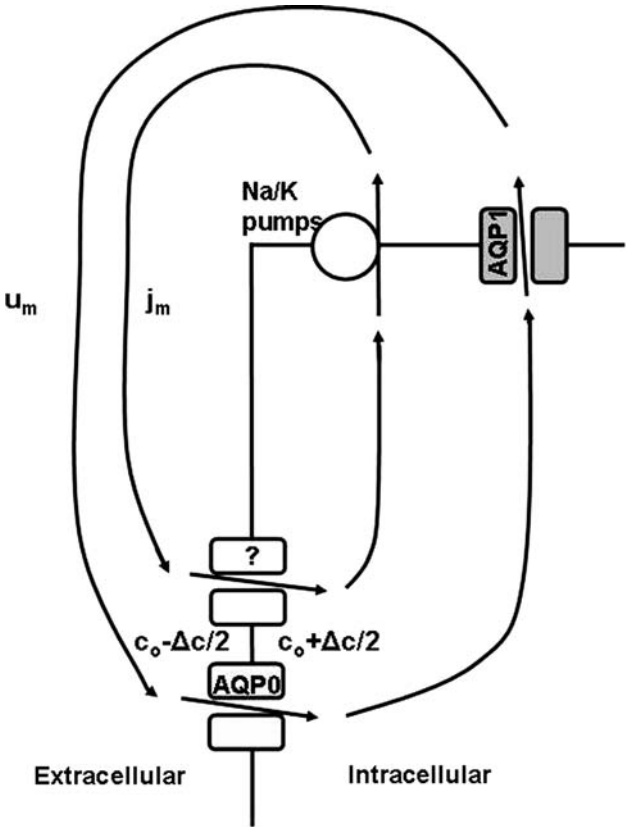

Fig. 4 Circulation of solute and fluid. As described for Figure 3, a net flux of sodium, j_m (moles/cm^2/s), enters the lens along the extracellular spaces, crosses into the fiber cells and then flows back to the surface from cell to cell via gap junctions. The circulation of sodium generates small transmembrane osmotic gradients, Δc (moles/cm^3), which cause a fluid flux, u_m (cm/s), to follow the solute flux

ute/solvent coupling through osmosis (Mathias & Wang, 2005). When a standing current is flowing, fluid will also move; the question is how much fluid will move and whether this movement will be physiologically relevant. In biological tissues where all fluxes are generated by transmembrane transport, this question reduces to how large the membrane water permeability is relative to solute flux. Mathias & Wang (2005) showed that the dimensionless ratio $(j_m/c_o)/(p_m c_o)$ must be small, where j_m (moles/cm^2/s) is solute flux, p_m [(cm/s)/(mole/cm^3)] is membrane water permeability and c_o = 300 x 10^{-6} (moles/cm^3) is the osmolarity of mammalian plasma. Varadaraj et al. (1999, 2005) measured the membrane water permeability of fiber cells from frog, rabbit and mouse lenses and found values that indicated the above ratio is about 10^{-4}, so fluid flow should approach its maximal limit of isotonic transport (*see* equation 8).

Fischbarg et al. (1999) reported that monolayers of cultured lens epithelial cells from bovine or mouse actively transported fluid in the basolateral to apical direction, which in the intact organ would be directed toward the lens core. They also observed fluid transport in the same direction when a rabbit lens was placed in an Ussing-like chamber that blocked the equatorial exit path.

Candia & Alverez (2006) reviewed their work on the bovine lens, where the circulating current is much less symmetric than in rabbit, rat or frog lenses, with the majority of the inward current flowing at the anterior pole. They also measured fluid transport and found it followed the same pattern. Thus, several direct measurements support the presence of fluid transport in the same pattern as the circulating currents. However, as described in the following section, the methodology used for intact lens studies may have significantly reduced the amount of fluid movement.

Mathias et al. (1997) modeled fluid and Na^+ moving into the lens strictly along the extracellular spaces. This is likely to be true within the fiber cell mass, but the work by Fischbarg et al. (1999) on isolated tissue cultured lens epithelium suggests the initial entry across the epithelial layer at the anterior surface is transcellular, as is the case in other fluid-transporting epithelia. If so, the fluxes would become extracellular only after they exit the epithelium. This path is consistent with transport by other epithelia which have tight junctions at their apical side; however, there have been questions on whether or not the lens epithelium has tight junctions (Goodenough, Dick & Lyons, 1980).

Mechanism of generating fluid transport

Most epithelia transport in the open circuit state, so there must be an electrically neutral transepithelial flux of NaCl to generate fluid transport. The lens is unique in that the salt transport is in the short circuit state with the extracellular solutions at the polar and equatorial surfaces being at the same voltage. Thus, at steady state, each Na^+ that crosses the membrane is replaced by the Na^+ behind it, so at no point in the loop is the steady-state Na^+ concentration changing. To set up this standing circulation, as Na^+ is pulled by its electrochemical gradient into a fiber cell, there is depletion of Na^+ from the extracellular space and accumulation within the fiber cell. This separation of charge generates a negative voltage in the extracellular space and moves the resting voltage in the cell somewhat more positive. As a consequence of these standing voltages, Cl^- tends to be depleted in the extracellular space and accumulates in the cell, even though it is not necessarily crossing the membrane. This standing transmembrane gradient of NaCl (Δc in Fig. 4) pulls water across the membrane to follow the flow of Na^+. As described previously, there is some modulation of the net transmembrane solute flux, j_m (moles/cm^2/s), due to Cl^- flux, but even in the complete absence of Cl^- movement, a circulation of just Na^+ could set up a circulation of fluid. Fischbarg et al. (1999) and Candia & Alverez (2006) used Ussing-like chambers, which open circuit the lens surfaces; hence, only electrically neutral NaCl can flow. Thus, the Na^+ can move no faster than Cl^-, which is close to electrochemical equilibrium, and the flux of Na^+ would be much less than that in the short circuit state. Accordingly, the fluid flux is also expected to be much less than in a free standing (short circuit) lens.

The transmembrane flow of water depends on the membrane water permeability (p_m, cm/s/M) times the osmotic gradient:

$$u_m = p_m \Delta c \tag{7}$$

If p_m is doubled, u_m will increase but will not double because the increase in water flow sweeps away some of the salt and reduces Δc. In the limiting case where $p_m \rightarrow \infty$ and $\Delta c \rightarrow 0$, the maximum fluid flow velocity is given by its isotonic limit (Mathias & Wang, 2005):

$$\textit{Isotonic transport} : u_m = j_m/c_o \tag{8}$$

The concentration of the transported solution is given by the transmembrane solute:water flux ratio, which is c_o in equation 8. The name ''isotonic transport'' is given because the bathing solutions and transported solution have the same tonicity. While the isotonic water flow velocity given in equation 8 cannot be attained, model calculations in Mathias & Wang (2005) suggest fluid transport in the lens will be within a few percent of isotonic.

The role of fluid transport

In general, an uncharged solute will move into and out of the lens through a combination of diffusion and convection. The time constant for diffusion depends on distance squared, whereas that for convection depends linearly on distance; hence, diffusion always dominates over short distances, whereas convection always dominates when the distance scale is long. To determine the physiological significance of each, we have to define the length scale of interest. An accurate comparison would require solving a set of rather intractable partial differential equations describing the circulating fluxes in the lens. Even approximate solutions to these equations are quite complex (Mathias et al., 1997). A simpler approach is to select a length scale and then compare the time constants for simple diffusion *vs.* convection.

If one analyzes a simple chamber with constant inflow and outflow, the time constant to change the composition of the fluid in the chamber is given by its volume divided by the rate of inflow. This would be the time constant for the change in concentration through convection of solute. We can think of the intracellular and extracellular compartments of the lens as being similar to such a chamber, so we need to estimate the rate of inflow.

Electrophysiological studies of the rat lens have provided reasonable estimates of j_{Na} and j_{Cl}, so we can estimate $j_m = j_{Na} + j_{Cl} = 10^{-12}$ moles/cm^2/s, which is relatively uniform regardless of depth (Baldo & Mathias, 1992; Mathias et al., 1985). Assuming near isotonic transport, this will generate a transmembrane fluid flow velocity of $u_m = j_m/c_o = 3.3 \times 10^{-9}$ cm/s, where $c_o = 300 \times 10^{-6}$ moles/cm^3. For a rat lens of radius $a = 0.2$ cm, the total fluid flow will be

$$U_{Total} = \frac{4}{3}\pi a^3 \frac{S_m}{V_T} u_m = 0.7x10^{-6}\, cm^3/s \qquad (9)$$

The time constant to clear the extracellular fluid compartment is given by the lens extracellular volume divided by U_{Total}, which is just 8 min. The Einstein relationship predicts the time constant for diffusion to the center of a sphere of radius a (cm), given by $a^2/(6D_e)$. The diffusion coefficient of glucose is about 5×10^{-6} cm^2/s; however, diffusion into the extracellular spaces within the lens depends on the tortuosity factor $\tau = 0.25$, as derived from equation 3. The time constant for diffusion into the extracellular spaces is therefore 1.5 h, whereas the time constant for convection to turn over the extracellular solution is 8 min. A realistic model of glucose movement into the lens would require a much more complex calculation that takes into account the rate of uptake by the fiber cells. Nevertheless, the above simple calculation illustrates the significant advantage of convection in the delivery of glucose to central fiber cells.

The above calculations were for the entire lens, so the length scale was the lens radius a. For sufficiently small length scales, diffusion will always dominate convection, so it is also of interest to estimate the distance into the lens at which diffusion and convection contribute equally to the delivery of glucose. We can calculate the time constant for fluid inflow to turn over the extracellular volume surrounding an outer shell of fiber cells of thickness Δr $[(4\pi a^2 \Delta r V_e/V_T)/U_{Total}]$, then set this equal to the time constant for one dimensional diffusion ($\Delta r^2/2D_e$) into the same volume. The result is $\Delta r = 180$ μm, or about 60 cell layers. Hence, for the outer fiber cells fewer than 60 cell layers from the surface, diffusion will be more effective than convection in the delivery of glucose; but for fiber cells deeper into the lens, convection becomes progressively more important.

The intracellular fluid flow velocity varies from a maximum angular average of $U_{Total}/(4\pi a^2) = 0.6$ μm/min at the lens surface to 0 μm/min at the lens center. Thus, the intracellular fluid flow velocity is quite slow and will be difficult to detect. However, with a length scale of the lens radius, diffusion is also very slow, so convection does have a potential impact on the movement of waste products from the lens center to surface. Intracellular diffusion, like current flow, must move through gap junctions. The effective radial intracellular resistivity is about 60-fold greater than that of cytoplasm. If we assume the diffusion coefficient is reduced by the same factor, then for a small solute whose diffusion coefficient is on the order of 10^{-5} cm^2/s, the effective intracellular diffusion coefficient would be $D_i = 1.7 \times 10^{-7}$ cm^2/s. The time constant to clear the intracellular compartment is 11 h for diffusion *vs.* 13 h for convection. Thus, both can potentially have an impact. However, in order for solute to move from cell to cell by convection, fluid and solute must share the same cell-to-cell path. The only known path that could fulfill this role is gap junctions. Although gap junction channels are thought to be capable of carrying water, for near isotonic transport, each channel would have to carry 183 water molecules with each ion. No one has demonstrated that gap junctions are capable of carrying such a large fluid flux, so this remains an unanswered question.

Lens water channels

Membrane water permeability is enhanced by a family of integral membrane proteins called the aquaporins (AQPs). A functional water channel is formed by the oligomerization of four AQPs, though each subunit has its own pore that is permeable to water and some neutral solutes but not to ions. Preston & Agre (1991) discovered the first such

channel (AQP1) in red blood cell membranes. AQP1 is also expressed in the lens epithelium but degraded at the E-DF transition and replaced by AQP0 (initially known as MIP). The abruptness and completeness of this transition (Varadaraj et al., 2005) suggest AQP0 has some specific role in fiber cell homeostasis. Knockout of AQP0 supports this idea since these lenses have degenerate fiber cells and opacify (Al-Ghoul et al., 2003; Shiels et al., 2001).

Exogenous expression of cloned AQP0 in *Xenopus* oocytes produced functional water channels (Mulders et al., 1995; Kushmerick et al., 1995; Chandy et al., 1997). Varadaraj et al. (1999) showed that fiber cell membranes have significant water permeability. They also showed that water permeability was greatly reduced in lenses from mice that expressed an AQP0 mutant protein unable to traffic to the plasma membrane. Subsequently, Shiels et al. (2001) found that fiber cell membrane water permeability was similarly reduced in AQP0 knockout lenses. Varadaraj et al. (1999) reported that water permeability of isolated lens epithelial cells was about fourfold larger than that of fiber cells. Moreover, epithelial cell membrane water permeability was mercury-sensitive, a property of AQP1 but not AQP0. Chandy et al. (1997), using freeze fracture electron microscopy to count the number of AQP channels in connection with water permeability measurements in oocytes, estimated AQP1 has about a 40-fold higher single-channel water permeability than AQP0. However, the water permeability of AQP0 was subsequently shown to be regulated, so it is not solely determined by the number of channels.

When exogenously expressed in oocytes, the water permeability of AQP0 was increased by about threefold in low external pH or low $[Ca^{2+}]_i$ and the calcium effect was shown to be calmodulin-dependent (Nemeth-Cahalan & Hall, 2000; Nemeth-Cahalan, Kalman & Hall, 2004). AQP0 water permeability in fiber cell membranes had the same pH effects, but the calcium/calmodulin effect was opposite: high rather than low intracellular calcium caused about a threefold increase that depended on calmodulin (Varadaraj et al., 2005). In a recent conference abstract, Kalman et al. (2006b) reported that the calcium/calmodulin effect in oocytes could be reversed to be the same as in lens fibers by replacing serine 235 with a phosphomimetic residue, which is presumably not phosphorylated in oocytes but is phosphorylated in the lens.

Upregulation of AQP0 water permeability by elevated internal calcium might be relevant in the lens since Gao et al. (2004) suggested that Ca^{2+} circulates in a manner similar to Na^+. Furthermore, they recorded a diffusion gradient in which the $[Ca^{2+}]_i$ is higher in central fiber cells than in peripheral cells, where active transport takes place. Gonen et al. (2004a,b, 2005) showed that the cleaved form of AQP0 in the lens core tends to form plaques in which the channels are closed. Thus, the amount of AQP0 that can function as a water channel is reduced in central fibers but might be compensated by the elevated $[Ca^{2+}]_i$, which might increase the permeability of remaining channels and maintain a more uniform overall water permeability. For technical reasons, it has not been possible to make water permeability measurements in membranes from central fibers. However, Kalman et al. (2006a) created a mouse that expressed both wild-type and mutant AQP0, and the lenses from these mice developed nuclear cataracts. Exogenous expression of the two proteins showed a normal value of membrane water permeability, but calcium regulation was lost, suggesting the possibility that cataracts were caused by the lack of calcium regulation. The mechanism of regulating the water permeability of AQP0 and the physiological role of regulation are interesting issues that await further experimentation.

Lens Cell Volume Regulation

Cells maintain volume by having a negative resting voltage to inhibit the influx of Cl^-. Thus, ion concentrations in most cells are maintained in a steady state whereas water is in equilibrium across the cell membrane. Because of the circulating ionic currents in the lens, there are radial voltage gradients in both the intracellular compartment (ψ_i, mV) and the extracellular spaces (ψ_e, mV); hence, there is no single resting voltage. Figure 5b sketches typical center-to-surface voltage gradients that have been recorded in several types of lenses (Mathias et al., 1997; Gong et al., 1998; Baldo et al., 2001; Martinez-Wittinghan et al., 2004). The transmembrane voltage is given by $\psi_i - \psi_e$, which varies from around –30 mV in the lens center to –70 mV in surface cells, at least in small lenses from rodents and frogs. Furthermore, water is not in static equilibrium; rather, it is in a dynamic steady state in which the amount of water entering each cell is balanced by the water leaving that cell. Despite this dynamic steady state, membrane water permeability is sufficiently high that the osmolarity of the intracellular compartment and extracellular spaces is expected to be relatively uniform (Mathias & Wang, 2005).

If Cl^- is the only anion, then it must contribute half the extracellular osmolarity and some smaller fraction of the intracellular osmolarity; hence, the Nernst potential, E_{Cl}, will be relatively uniform. Based on an extracellular concentration of 150 mM and an intracellular concentration of around 20 mM (Paterson & Eck, 1971), $E_{Cl} \approx -50$ mV, as shown in Figure 5b. The transmembrane voltage therefore crosses E_{Cl} such that there is an outward Cl^-flux (j_{Cl}) in the cortex and an inward j_{Cl} in the more central fiber cells. This spatial change in direction for Cl^- fluxes has important consequences for fiber cell volume regulation and the maintenance of lens transparency.

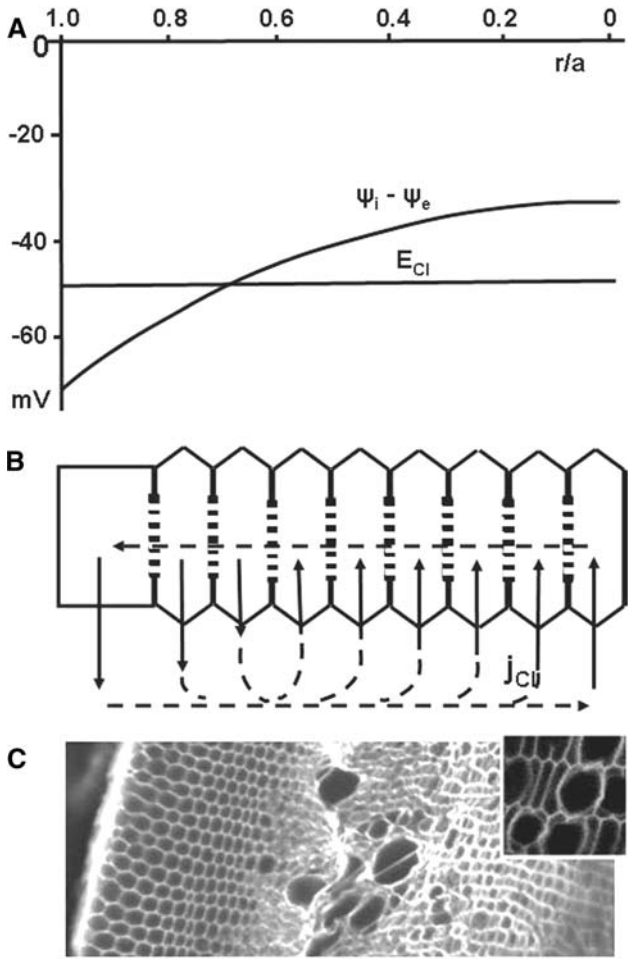

Fig. 5 Chloride fluxes in the lens. The direction of j_{Cl} changes where the fiber cell transmembrane voltage becomes more positive than the Nernst potential for chloride. (**a**) The fiber cell transmembrane potential varies as a function of radial distance into the lens. By superimposing a plot of the Nernst potential for Cl^- (E_{Cl}), model calculations suggest that in peripheral fiber cells Cl^- efflux is favored while in deeper fiber cells Cl^- influx occurs. (**b**) Schematic diagram depicting the circulating flux of Cl^- ions proposed to be generated by the gap junction-mediated coupling of Cl^- influx in deeper fiber cells and Cl^- efflux in peripheral fiber cells. (**c**) An equatorial section taken from a rat lens organ cultured under isotonic conditions for 18 h in the presence of 100 μM of the Cl^- channel inhibitor NPPB. Membranes are labeled with the wheat germ agglutinin (Young et al., 2000). Blocking Cl^- fluxes with NPPB resulted in two morphologically distinct zones of damage. Initially, extracellular spaces between fiber cells (*inset*), located in a discrete zone some 100–150 μm in from the capsule, expanded and by 18 h developed into a zone of extensive tissue breakdown. In contrast, peripheral fiber cells exhibited cell swelling. This pattern of a peripheral intracellular volume increase but deeper extracellular volume increase is consistent with the model of a circulating chloride flux presented in **a** and **b**

Lenses placed in hypotonic medium initially swell but then undergo a regulatory volume decrease (RVD) via the loss of K^+ and Cl^- ions and obligatory water loss (Patterson, 1980). In other cell types, the efflux of KCl associated with the RVD is mediated by the activation of K^+ and Cl^- channels (Niemeyer, Cid & Sepulveda, 2001; Sardini et al., 2003) and/or potassium chloride cotransporters (KCCs) (Lauf & Adragna, 2000). The relative contributions of Cl^- channels and KCCs to volume regulation have been examined in cultured rat lenses using reagents that modulated the activity of Cl^- transport proteins (Chee, Kistler & Donaldson, 2006; Merriman-Smith et al., 2002; Tunstall et al., 1999; Webb et al., 2004; Young et al., 2000). Lenses exposed to the Cl^- channel inhibitor 5-nitro-2-(3-phenylpropylamino)benzoic acid (NPPB) increased their volume and exhibited light scattering (Tunstall et al., 1999). Thus, under normal isotonic conditions, the lens has a constitutively active Cl^- flux, which regulates fiber cell volume and maintains lens transparency.

Histological analysis of NPPB-treated lenses cultured under isotonic conditions revealed that blocking Cl^- channels induces two spatially distinct tissue damage phenotypes (Young et al., 2000). Initially, a band of extracellular space dilations, located ~150 μm in from the capsule (Fig. 5c, inset), developed and progressed to more extensive tissue breakdown (Fig. 5c). Subsequently, a zone of cell swelling developed in peripheral tissue. Since cells will swell when Cl^- efflux is blocked whereas the spaces between cells will expand when Cl^- influx is blocked, the NPPB-induced zones of peripheral cell swelling and deeper accumulations of fluid between cells provided evidence for a circulating Cl^- flux, as predicted by the circulation model (Fig. 5a,b) of the normal lens.

Further experiments with lenses cultured under isotonic conditions and using more specific lower concentrations of NPPB, the KCC inhibitor [(dihydronindenyl)oxy]alkanoic acid (DIOA) or the Na^+, K^+, 2 Cl^-cotransporter (NKCC) blocker bumetanide also produced spatially distinct damage phenotypes (Chee et al., 2006). These series of experiments not only supported the contribution of a circulating Cl^- flux to the maintenance of steady-state lens volume but also indicated that this flux is mediated by interplay between a variety of Cl^- channels and transporters (Fig. 6). The primary effect of blocking Cl^- influx via NKCC with bumetanide was the formation of a localized zone of extracellular space dilations between inner cortical fiber cells. In contrast, the predominant effect of inhibiting KCC with DIOA was the induction of cellular swelling in peripheral fiber cells, indicating that KCCs mediate Cl^- efflux in these cells. With DIOA, some deeper extracellular space dilations were also observed, suggesting that KCC may also contribute to Cl^- influx in deeper fiber cells or alternatively that DIOA blocks some other Cl^- influx pathway. To distinguish between these possibilities, additional morphological experiments were performed on organ cultured lenses exposed to *N*-ethylmaleimide (NEM), an activator of KCC (Lauf & Adragna, 2000). NEM invoked cell shrinkage in peripheral cells but cell swelling in

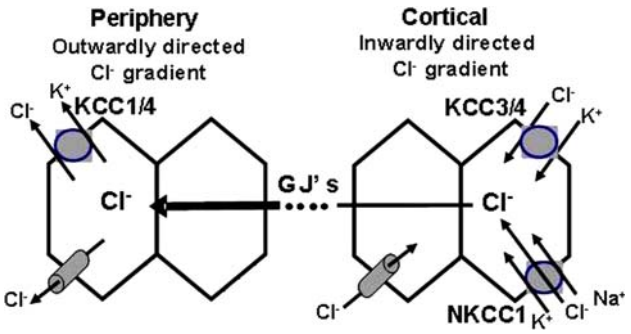

Fig. 6 Schematic diagram summarizing our current understanding of the cellular mechanisms mediating Cl^- fluxes in the rat lens. *Cylinders* are meant to indicate Cl^- channels, whose molecular identity is not yet known. KCC represents the K^+, Cl^- cotransporter. NKCC represents the Na^+, K^+, 2 Cl^- cotransporter

deeper fiber cells, consistent with the idea that KCC indeed plays a role in both Cl^- efflux and influx in the different regions of the lens (Chee et al., 2006). These results are summarized in Figure 6.

So far, we have shown how biophysical calculations have led to informed experimentation with pharmacological reagents – together generating an emerging molecular model for the maintenance of steady-state lens volume. The pharmacologically induced changes in the morphology of lenses have been interpreted with reference to the lens circulation system. This model has gained further support from molecular localization studies and electrophysiological functional experiments performed on isolated fiber cells. Chee et al. (2006) have shown that both KCC and NKCC1 are expressed in the rat lens. In the case of KCC, the three isoforms detected (KCC1, KCC3 and KCC4) not only are expressed in a differentiation-dependent manner but exhibit isoform-specific changes in their subcellular distribution in response to changes in fiber cell volume. Fiber cell swelling evoked either isosmotically by the DIOA-induced blockage of Cl^- efflux in peripheral fiber cells or via hypo-osmotic challenge caused a noticeable increase in membrane insertion of KCC1 and KCC4 but not KCC3. This observed translocation of KCCs indicates that the ability of KCC to regulate fiber cell volume is a dynamic process that responds to lens stress.

While the molecular identity of Cl^-channels in the lens remains unknown, patch-clamp experiments on isolated fiber cells have allowed their functional characterization. By relating fiber cell length to fiber cell position (cell layers) in lens sections, Webb et al. (2004) were able to show that isolated fiber cells longer than 120 μm originated from the zone of extracellular space dilations. This type of cell exhibited an outwardly rectifying chloride conductance that was blocked by Cl^- channel inhibitors. These cells also exhibited a lypotrophic anion selectivity sequence ($I^- > Cl^-$), reminiscent of volume-sensitive Cl^- conductances seen in many cell types. In contrast, shorter fiber cells isolated from the lens periphery lacked constitutively active Cl^- channels. These are the same cells that became swollen upon treatment of isotonic lenses with DIOA (Donaldson et al., 2005), suggesting a more important role for transporters than channels.

Nutrient and Antioxidant Uptake

Mature fiber cells lack cellular organelles, but they still require nutrients for anaerobic metabolism and antioxidants to maintain lens transparency. The circulation system may carry these nutrients and antioxidants into the lens core via an extracellular route. If so, fiber cells need membrane transporters to accumulate the molecules delivered to them by the circulation system.

Molecular studies have indeed shown that fiber cells express transporters that mediate the uptake of glucose (Merriman-Smith et al., 2003; Merriman-Smith, Donaldson & Kistler, 1999) and amino acids involved in the synthesis of the antioxidant glutathione (GSH) (Li et al., 2007; Lim et al., 2005, 2006). Furthermore, immunocytochemical localization of these transporters suggests that differences exist in the complement of transporters expressed in the cortex and core of the lens (Fig. 7). Since fiber cells are not capable of *de novo* protein synthesis, the old dogma was that they had to utilize the same complement of membrane transport proteins for the life of the animal. New data suggest this is not true. The outer DF express plasma membrane transport proteins that are appropriate for that location but also synthesize transport proteins that are more appropriate for the environment in the MF. These (MF) transport proteins appear to be stored in a pool of intracellular vesicles, which, at the appropriate stage of fiber differentiation, fuse with the plasma membrane and insert a new complement of membrane transporters.

The facilitated glucose transporter GLUT1 is expressed in the lens epithelium; however, at the E-DF transition, immunostaining for GLUT1 is lost and staining for GLUT3 as well as the sodium-dependent glucose transporter SGLT2 is observed. GLUT3 is inserted into the plasma membranes of DF, but plasma membrane staining for SGLT2 is not observed until the DF lose their organelles and become MF. The SGLT family has a higher affinity for glucose than the GLUT family, so insertion of SGLT in the membranes of interior fiber cells may allow uptake of glucose from extracellular solution that has been depleted of glucose due to uptake by more cortical cells.

GSH is synthesized from the amino acids cysteine, glycine and glutamate. Cysteine is generally the rate-limiting substrate (Beutler, 1989; Burdo, Dargusch & Schubert, 2006; Davis et al., 1993; Deneke & Fanburg, 1989).

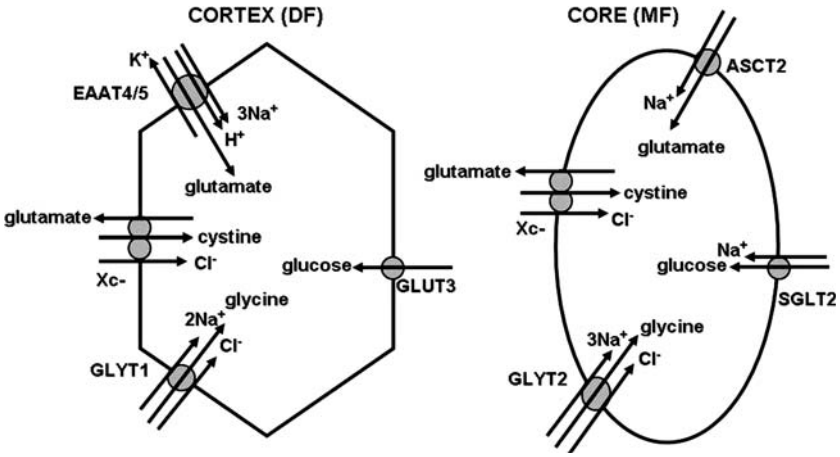

Fig. 7 Schematic of regional differences in the expression of transporters involved in the uptake of glucose and amino acids. *DF* differentiating fiber, *MF* mature fiber, *ASCT* alanine serine-cysteine Na^+-dependent cotransporter family, *EAAT* Na^+-dependent excitatory amino acid transporter family, *Xc-* cystine/glutamate exchanger, *GLYT* Na^+-dependent glycine cotransporter family, *GLUT* facilitative glucose transporter family, *SGLT* Na^+-dependent glucose cotransporter family

Cysteine is a sulfur-containing amino acid that is inherently unstable in free solution. Cystine, the dimeric oxidized form of cysteine, is more stable and more abundant than cysteine in the aqueous humor (Mackic et al., 1997; Wang & Cynader, 2000). In the lens core, where little if any GSH synthesis takes place, cysteine may act as a small molecular weight antioxidant by maintaining the free sulfhydryl groups of proteins in their reduced state (Lou, 2003). By analogy to the GSH/GSSG (reduced GSH) cycle (Reddy, 1990), a similar antioxidant role for cysteine/cystine may exist.

In the rat lens, uptake of cystine from the aqueous humor is mediated by the amino acid transporter Xc- (Lim et al., 2005), which exchanges extracellular cystine for intracellular glutamate (Fig. 7). This exchange system relies on the maintenance of a high intracellular glutamate concentration, and in other tissues this is mediated by members of the X_{AG} amino acid transport family (McBean, 2002; McBean & Flynn, 2001). The X_{AG} transporters are a multigene family of Na^+-dependent amino acid transporters, which include the excitatory amino acid transporters (EAAT1-5) and the alanine serine cysteine transporters (ASCT1-2) (Gegelashvili & Schousboe, 1997). In the rat lens, Xc- is expressed in combination with different members of the X_{AG} family. In the outer cortex, Xc- expression was shown to overlap with EAAT4/5 expression, while in the core, Xc- expression colocalized with ASCT2 expression (Lim et al., 2005; Lim et al., 2006). The observed switch in glutamate uptake mechanisms from EAAT4/5 to ASCT2 may reflect the ability of ASCT2 to preferentially accumulate glutamate at low intracellular pH (Utsunomiya-Tate, Endou & Kanai, 1996), which prevails in the lens core (Baldo & Mathias, 1992).

Based on immunostaining, the glycine transporter GLYT1 is expressed exclusively in the plasma membranes of DF (Lim et al., 2006). However, Lim (*personal communication*) has found evidence for glycine uptake in the lens core. An antibody for GLYT2 provided immunostaining evidence that GLYT2 is present in the plasma membranes of MF and, thus, may mediate glycine uptake in the core. Though the glycine study is in a more preliminary state than those for cysteine and glutamate, the pattern appears to be the same: there are fiber cell transporters that differ from epithelial cell transporters, and the complement of fiber cell transporters in the DF differs from that in the MF. This pattern strongly suggests an extracellular delivery pathway, consistent with the circulation system delivering the solutes.

A Model for Nuclear Cataract

As indicated in Figure 7, fiber cells express a variety of transporters that either directly or indirectly utilize energy stored in the Na^+ gradient to drive the accumulation of nutrients against their concentration gradients. The Na^+ gradient is ultimately maintained by the active removal of Na^+ at the lens equatorial surface. Thus, in addition to generating the circulating ion fluxes that underpin the convective delivery of nutrients to deeper fiber cells, Na^+ efflux at the lens surface serves to maintain the transmembrane Na^+ gradient utilized by secondary active transporters to accumulate nutrients in the lens core. One assumes, therefore, that any dissipation of the Na^+ gradient in the core of the lens will reduce nutrient uptake in this region. Interestingly, age-related nuclear (ARN) cataract is associated with a progressive fall in cysteine and GSH levels in the core but not the cortex (Rathbun & Murray, 1991; Sweeney & Truscott, 1998). This suggests that, with advancing age, the ability of the circulation system to maintain appropriate nutrient and antioxidant levels in the lens core declines and exposes crystallin proteins in the lens core to the oxidative damage that may precipitate cataract formation.

While cumulative oxidative damage to any component of the circulation system (surface Na/K pumps, fiber cell ion/water channels or fiber cell gap junctions) could lead to

cataract formation, ARN cataract may become more likely simply due to an inability of the circulation system to compensate for the decades of continuing lens growth. The lens grows throughout life by laying down new fiber cells that internalize the older cells. Since each additional fiber cell layer will contribute to the overall Na^+ leak, an age-dependent increase in passive Na^+ influx occurs, which necessitates an increase in active Na^+ efflux at the lens surface to maintain ionic homeostasis. The surface area of the lens available for mediating Na^+ efflux, however, does not increase at the same rate (see equation 5). This line of reasoning is supported by measurements in human lenses which have depolarized voltages and increased intracellular Na^+ with advancing age (Duncan et al., 1989). This age-dependent decline in the Na^+ gradient continues throughout life and may eventually contribute to initiation of ARN cataract.

If this interpretation is correct, therapeutic interventions to prevent the oxidative damage that initiates ARN cataract should focus on enhancing the activity of the circulation system. Stimulation of the circulation system in the ageing lens will not only increase the delivery of nutrients and antioxidants to the lens core but also enhance their uptake by restoring the Na^+ gradient utilized by the transporters expressed in this region of the lens. This mechanistic hypothesis for the onset of ARN cataract illustrates the potential benefits of pursuing basic research into the cellular and molecular mechanism responsible for lens transparency. Novel insights into the initiation of lens cataract highlight the value of integrative functional models in furthering our understanding of organ function and the potential for innovative new drug design.

Acknowledgement This work was supported by National Institutes of Health grant EY06391 and The Health Research Council of New Zealand. We thank Dr. Linda Musil for a critical reading of a preliminary version.

References

Al-Ghoul KJ, Kirk T, Kuszak AJ, Zoltoski RK, Shiels A, Kuszak JR (2003) Lens structure in MIP-deficient mice. Anat Rec A Discov Mol Cell Evol Biol 273:714–730

Baldo GJ, Mathias RT (1992) Spatial variations in membrane properties in the intact rat lens. Biophys J 63:518–529

Baldo GJ, Gong X, Martinez-Wittinghan FJ, Kumar NM, Gilula NB, Mathias RT (2001) Gap junctional coupling in lenses from alpha(8) connexin knockout mice. J Gen Physiol 118:447–456

Ball LE, Garland DL, Crouch RK, Schey KL (2004) Post-translational modifications of aquaporin 0 (AQP0) in the normal human lens: spatial and temporal occurrence. Biochemistry 30:9856–9865

Bassnett S (2002) Lens organelle degradation. Exp Eye Res 74:1–16

Berthoud VM, Cook AJ, Beyer EC (1994) Characterization of the gap junction protein connexin56 in the chicken lens by immunofluorescence and immunoblotting. Invest Ophthalmol Vis Sci 35:4109–4117

Beutler E (1989) Nutritional and metabolic aspects of glutathione. Annu Rev Nutr 9:287–302

Burdo J, Dargusch R, Schubert D (2006) Distribution of the cystine/glutamate antiporter system Xc- in the brain, kidney and duodenum. J Histochem Cytochem 54:549–557

Candia OA, Alverez JL (2006) Water and ion transport in ocular tissues. Physiol Minirev 1:48–57

Candia OA, Zamudio AC (2002) Regional distribution of the Na^+ and K^+ currents around the crystalline lens of rabbit. Am J Physiol 282:C252–C262

Chandy G, Zampighi GA, Kreman M, Hall JE (1997) Comparison of the water transporting properties of MIP and AQP1. J Membr Biol 159:29–39

Chee K-SN, Kistler J, Donaldson PJ (2006) Roles for KCC transporters in the maintenance of lens transparency. Invest Ophthalmol Vis Sci 47:673–682

Cooper K, Gates P, Rae JL, Dewey J (1990) Electrophysiology of cultured human lens epithelial cells. J Membr Biol 117:285–298

Cooper K, Rae JL, Dewey J (1991) Inwardly rectifying potassium current in mammalian lens epithelial cells. Am J Physiol 261(Pt 1):C115–C123

Cooper K, Watsky M, Rae J (1992) Potassium currents from isolated frog lens epithelial cells. Exp Eye Res 55:861–868

Dahm R, van Marle J, Prescott AR, Quinlan RA (1999) Gap junctions containing alpha8-connexin (MP70) in the adult mammalian lens epithelium suggests a re-evaluation of its role in the lens. Exp Eye Res 69:45–56

Davis MA, Wallig MA, Eaton D, Borroz KI, Jeffery EH (1993) Differential effect of cyanohydroxybutene on glutathione synthesis in liver and pancreas of male rats. Toxicol Appl Pharmacol 123:257–264

Delamere NA, Tamiya S (2004) Expression, regulation and function of Na,K ATPase in the lens. Prog Retin Eye Res 23:593–615

Deneke SM, Fanburg BL (1989) Regulation of cellular glutathione. Am J Physiol 257:L163–L173

DeRosa AM, Martinez-Wittinghan MJ, Mathias RT, White TW (2005) Intracellular communication in lens development and disease. In: Winterhager E (ed), Gap Junctions in Development and Disease. Berlin: Springer-Verlag, pp 173–195

Donaldson P, Kistler J, Mathias RT (2001) Molecular solutions to mammalian lens transparency. News Physiol Sci 16:118–123

Donaldson PJ, Grey AC, Merriman-Smith BR, Sisley AM, Soeller C, Cannell MB, Jacobs MD (2004) Functional imaging: new views on lens structure and function. Clin Exp Pharmacol Physiol 31:890–895

Donaldson PJ, Chee KN, Webb KF, Kistler J (2005) Spatially distinct Cl^- influx and efflux pathways interact to maintain lens volume and transparency. Invest Ophthalmol Vis Sci 46:1129

Duncan G, Hightower KR, Gandolfi SA, Tomlinson JGM (1989) Human lens membrane cation permeability increases with age. Invest Ophthalmol Vis Sci 30:1855–1859

Ebihara L (2003a) New roles for connexons. News Physiol Sci 18:100–103

Ebihara L (2003b) Physiology and biophysics of hemi-gap-junctional channels expressed in *Xenopus* oocytes. Acta Physiol Scand 179:5–8

Fischbarg J, Diecke FP, Kuang K, Yu B, Kang F, Iserovich P, Li Y, Rosskothen H, Koniarek JP (1999) Transport of fluid by lens epithelium. Am J Physiol 276:C548–C557

Gao J, Sun X, Martinez-Wittinghan FJ, Gong X, White TW, Mathias RT (2004) Connections between connexins, calcium, and cataracts in the lens. J Gen Physiol 124:289–300

Gao J, Sun X, Yatsula V, Wymore RS, Mathias RT (2000) Isoform-specific function and distribution of Na/K pumps in the frog lens epithelium. J Membr Biol 178:89–101

Garner MH, Horowitz J (1994) Catalytic subunit isoforms of mammalian lens Na,K-ATPase. Curr Eye Res 13:65–77

Geering K (2006) FXYD proteins; new regulators of Na-K-ATPase. Am J Physiol 290:F241–F250

Gegelashvili G, Schousboe A (1997) High affinity glutamate transporters: regulation of expression and activity. Mol Pharmacol 52:6–15

Gick GG, Hatala MA, Chon D, Ismail-Beigi F (1993) Na,K-ATPase in several tissues of the rat: tissue-specific expression of subunit mRNAs and enzyme activity. J Membr Biol 131:229–236

Gonen T, Cheng Y, Kistler J, Walz T (2004a) Aquaporin-0 membrane junctions form upon proteolytic cleavage. J Mol Biol 342:1337–1345

Gonen T, Cheng Y, Sliz P, Hiroaki Y, Fujiyoshi Y, Harrison SC, Walz T (2005) Lipid-protein interactions in double-layered two-dimensional AQP0 crystals. Nature 438:633–638

Gonen T, Sliz P, Kistler J, Cheng Y, Walz T (2004b) Aquaporin-0 membrane junctions reveal the structure of a closed water pore. Nature 429:193–197

Gong X, Baldo GJ, Kumar NM, Gilula NB, Mathias RT (1998) Gap junctional coupling in lenses lacking alpha3 connexin. Proc Natl Acad Sci USA 95:15303–15308

Goodenough DA, Dick JS 2nd, Lyons JE (1980) Lens metabolic cooperation: a study of mouse lens transport and permeability visualized with freeze-substitution autoradiography and electron microscopy. J Cell Biol 86:576–589

Gruijters WT, Kistler J, Bullivant S, Goodenough DA (1987) Immunolocalization of MP70 in lens fiber 16–17-nm intercellular junctions. J Cell Biol 104:565–572

Jacobs MD, Soeller C, Sisley AM, Cannell MB, Donaldson PJ (2004) Gap junction processing and redistribution revealed by quantitative optical measurements of connexin46 epitopes in the lens. Invest Ophthalmol Vis Sci 45:191–199

Kalman K, Nemeth-Cahalan KL, Froger A, Hall JE (2006a) AQP0-LTR of the Cat(Fr) mouse alters water permeability and calcium regulation of wild type AQP0. Biochim Biophys Acta 1758:1094–1099

Kalman K, Nemeth-Cahalan K, Froger A, Hall JE (2006b) Role of the AQP0 C-terminus in calcium-mediated regulation of water permeability. Association for Research in Vision & Ophthalmology Annual meeting, Ft. Lauderdale, FL. Abstract 5421. http://www.arvo.org

Kistler J, Bullivant S (1987) Protein processing in lens intercellular junctions: cleavage of MP70 to MP38. Invest Ophthalmol Vis Sci 28:1687–1692

Kistler J, Kirkland B, Bullivant S (1985) Identification of a 70,000-D protein in lens membrane junctional domains. J Cell Biol 101:28–35

Kushmerick C, Rice SJ, Baldo GJ, Haspel HC, Mathias RT (1995) Ion, water and neutral solute transport in *Xenopus* oocytes expressing frog lens MIP. Exp Eye Res 61:351–362

Kuszak JR, Bertram BA, Macsai MS, Rae JL (1984) Sutures of the crystalline lens: a review. Scanning Electron Microsc (Pt 3):1369–1378

Kuszak JR, Rae JL (1982) Scanning electron microscopy of the frog lens. Exp Eye Res 35:499–519

Lauf PK, Adragna NC (2000) K-Cl cotransport: properties and molecular mechanism. Cell Physiol Biochem 10:341–354

Le A-C, Musil LS (2001) A novel role for FGF and extracellular signal-regulated kinase in gap junction-mediated intercellular communication in the lens. J Cell Biol 154:197–216

Li L, Lim JC, Jacobs MD, Kistler J, Donaldson PJ (2007) Regional differences in cystine accumulation point to a sutural delivery pathway to the lens core. Invest Ophthalmol Vis Sci (in press)

Lim J, Lam YC, Kistler J, Donaldson PJ (2005) Molecular characterization of the cystine/glutamate exchanger and the excitatory amino acid transporters in the rat lens. Invest Ophthalmol Vis Sci 46:2869–2877

Lim J, Lorentzen KA, Kistler J, Donaldson PJ (2006) Molecular identification and characterization of the glycine transporter (GLYT1) and the glutamine/glutamate transporter (ASCT2) in the rat lens. Exp Eye Res 83:447–455

Lin JS, Fitzgerald S, Dong Y, Knight C, Donaldson P, Kistler J (1997) Processing of the gap junction protein connexin50 in the ocular lens is accomplished by calpain. Eur J Cell Biol 73:141–149

Lou MF (2003) Redox regulation in the lens. Prog Retin Eye Res 22:657–682

Mackic JB, Kannan R, Kaplowitz N, Zlokovic BV (1997) Low de novo glutathione synthesis from circulating sulfur amino acids in the lens epithelium. Exp Eye Res 64:615–626

Maisel H, Harding CV, Alcala JR, Breadley R (1981) The morphology of the lens. In: Bloemendal H (ed), Molecular and Cellular Biology of the Eye Lens. New York: Wiley, pp 49–83

Martinez-Wittinghan FJ, Sellitto C, White TW, Mathias RT, Paul D, Goodenough DA (2004) Lens gap junctional coupling is modulated by connexin identity and the locus of gene expression. Invest Ophthalmol Vis Sci 45:3629–3637

Mathias RT (1983) Effects of tortuous extracellular pathways on resistance measurements. Biophys J 42:55–59

Mathias RT (1985) Epithelial water transport in a balanced gradient system. Biophys J 47:823–836

Mathias RT, Rae JL (1985) Transport Properties of the lens. Am J Physiol Cell Physiol 249:C181–C190

Mathias RT, Cohen IS, Wang Y (2000) Isoform-specific regulation of the Na^+-K^+ pump in heart. New Physiol sci 15:176–180

Mathias RT, Rae JL, Baldo GJ (1997) Physiological properties of the normal lens. Physiol Rev 77:21–50

Mathias RT, Rae JL, Ebihara L, McCarthy RT (1985) The localization of transport properties in the frog lens. Biophys J 48:423–434

Mathias RT, Rae JL, Eisenberg RS (1979) Electrical properties of structural components of the crystalline lens. Biophys J 25:181–201

Mathias RT, Wang H (2005) Local osmosis and isotonic transport. J Membr Biol 208:39–53

McBean GJ (2002) Cerebral cystine uptake: a tale of two transporters. Trends Pharmacol Sci 23:299–302

McBean GJ, Flynn J (2001) Molecular mechanisms of cystine transport. Biochem Soc Trans 29:717–722

Menko SA (2002) Lens epithelial cell differentiation. Exp Eye Res 75:485–490

Merriman-Smith BR, Krushinsky A, Kistler J, Donaldson PJ (2003) Expression patterns for glucose transporters GLUT1 and GLUT3 in the normal rat lens and in models of diabetic cataract. Invest Ophthalmol Vis Sci 44:3458–3466

Merriman-Smith BR, Young MA, Jacobs MD, Kistler J, Donaldson PJ (2002) Molecular identification of P-glycoprotein: a role in lens circulation? Invest Ophthalmol Vis Sci 43:3008–3015

Merriman-Smith R, Donaldson P, Kistler J (1999) Differential expression of facilitative glucose transporters GLUT1 and GLUT3 in the lens. Invest Ophthalmol Vis Sci 40:3224–3230

Miller AG, Zampighi GA, Hall JE (1992) Single-membrane and cell-to-cell permeability properties of dissociated embryonic chick lens cells. J Membr Biol 128:91–102

Mulders SM, Preston GM, Deen PM, Guggino WB, van Os CH, Agre P (1995) Water channel properties of major intrinsic protein of lens. J Biol Chem 270:9010–9016

Nemeth-Cahalan KL, Hall JE (2000) pH and calcium regulate the water permeability of aquaporin 0. J Biol Chem 275:6777–6782

Nemeth-Cahalan KL, Kalman K, Hall JE (2004) Molecular basis of pH and Ca^{2+} regulation of aquaporin water permeability. J Gen Physiol 123:573–580

Niemeyer MI, Cid LP, Sepulveda FV (2001) K^+ conductance activated during regulatory volume decrease. The channels in Ehrlich cells and their possible molecular counterpart. Comp Biochem Physiol A Mol Integr Physiol 130:565–575

Parmelee JT (1986) Measurement of steady currents around the frog lens. Exp Eye Res 42:433–441

Paterson CA (1972) Distribution and movement of ions in the ocular lens. Doc Ophthalmol 31:1–28

Paterson CA, Delamere NA (2004) ATPases and lens ion balance. Exp Eye Res 78:699–703

Paterson CA, Eck BA (1971) Chloride concentration and exchange in rabbit lens. Exp Eye Res 11:207–213

Paterson CA, Neville MC, Jenkins RM 2nd, Nordstrom DK (1974) Intracellular potassium activity in frog lens determined using ion specific liquid ion-exchanger filled microelectrodes. Exp Eye Res 19:43–48

Patterson JW (1980) Volume regulation in rat lens. In: Red Blood Cell and Lens Metabolism. Amsterdam: Elsevier

Peskoff A (1979) Electric potential in cylindrical syncytia and muscle fibers. Bull Math Biol 41:183–192

Preston GM, Agre P (1991) Isolation of the cDNA for erythrocyte integral membrane protein of 28 kilodaltons: member of an ancient channel family. Proc Natl Acad Sci USA 88:11110–11114

Rae JL (1994) Outwardly rectifying potassium currents in lens epithelial cell membranes. Curr Eye Res 13:679–686

Rae JL, Rae JS (1992) Whole-cell currents from noncultured human lens epithelium. Invest Ophthalmol Vis Sci 33:2262–2268

Rae JL, Shepard AR (1998a) Ion transporters and receptors in cDNA libraries from lens and cornea epithelia. Curr Eye Res 17:708–719

Rae JL, Shepard AR (1998) Inwardly rectifying potassium channels in lens epithelium are from the IRK1 (Kir 2.1) family. Exp Eye Res 66:347–359

Rae JL, Shepard AR (1998c) Molecular biology and electrophysiology of calcium-activated potassium channels from lens epithelium. Curr Eye Res 17:264–275

Rae JL, Shepard AR (2000a) Kir2.1 potassium channels and corneal epithelia. Curr Eye Res 20:144–152

Rae JL, Shepard AR (2000b) Kv3.3 potassium channels in lens epithelium and corneal endothelium. Exp Eye Res 70:339–348

Rathbun WB, Murray DL (1991) Age-related cysteine uptake as rate-limiting in glutathione synthesis and glutathione half-life in the cultured human lens. Exp Eye Res 53:205–212

Reddy VN (1990) Glutathione and its function in the lens – an overview. Exp Eye Res 50:771–778

Robinson KR, Patterson JW (1982) Localization of steady currents in the lens. Curr Eye Res 2:843–847

Sardini A, Amey JS, Weylandt KH, Nobles M, Valverde MA, Higgins CF (2003) Cell volume regulation and swelling-activated chloride channels. Biochim Biophys Acta Biomembr 1618:153–162

Shepard AR, Rae JL (1998) Ion transporters and receptors in cDNA libraries from lens and cornea epithelia. Curr Eye Res 17:708–719

Shepard AR, Rae JL (1999) Electrically silent potassium channel subunits from human lens epithelium. Am J Physiol 277(Pt 1):C412–C424

Shiels A, Bassnett S, Varadaraj K, Mathias R, Al-Ghoul K, Kuszak J, Donoviel D, Lilleberg S, Friedrich G, Zambrowicz B (2001) Optical dysfunction of the crystalline lens in aquaporin-0-deficient mice. Physiol Genomics 7:179–186

Sweadner KJ (1989) Isozymes of the Na^+/K^+-ATPase. Biochim Biophys Acta 988:185–220

Sweeney MHJ, Truscott RJW (1998) An impediment to glutathione diffusion in older normal human lenses: a possible precondition for nuclear cataract. Exp Eye Res 67:587–595

Tamiya S, Dean WL, Paterson CA, Delamere NA (2003) Regional distribution of Na,K-ATPase activity in porcine lens epithelium. Invest Ophthalmol Vis Sci 44:4395–4399

Tunstall MJ, Eckert R, Donaldson P, Kistler J (1999) Localized fibre cell swelling characteristic of diabetic cataract can be induced in normal rat lens using the chloride channel blocker 5-nitro-2-(3-phenylpropylamino) benzoic acid. Ophthalmic Res 31:317–320

Utsunomiya-Tate N, Endou H, Kanai Y (1996) Cloning and functional characterization of a system ASC-like Na^+ dependent neutral amino acid transporter. J Biol Chem 271:14883–14890

Varadaraj K, Kushmerick C, Baldo GJ, Bassnett S, Shiels A, Mathias RT (1999) The role of MIP in lens fiber cell membrane transport. J Membr Biol 170:191–203

Varadaraj K, Kumari S, Shiels A, Mathias RT (2005) Regulation of aquaporin water permeability in the lens. Invest Ophthalmol Vis Sci 46:1393–1402

Wang XF, Cynader MS (2000) Astrocytes provide cysteine to neurons by releasing glutathione. J Neurochem 74:1434–1442

Webb KF (2006) Spatial variations in the membrane properties of differentiating fibre cells isolated from the rat lens. PhD diss, University of Auckland

Webb KF, Merriman-Smith BR, Stobie JK, Kistler J, Donaldson PJ (2004) Cl^- influx into rat cortical lens fiber cells is mediated by a Cl^- conductance that is not ClC-2 or -3. Invest Ophthalmol Vis Sci 45:4400–4408

Yin X, Gu S, Jiang JX (2001a) The development-associated cleavage of lens connexin 45.6 by caspase-3-like protease is regulated by casein kinase II-mediated phosphorylation. J Biol Chem 276:34567–34572

Yin X, Gu S, Jiang JX (2001b) Regulation of lens connexin 45.6 by apoptotic protease, caspase-3. Cell Commun Adhes 8:373–376

Young MA, Tunstall MJ, Kistler J, Donaldson PJ (2000) Blocking chloride channels in the rat lens: localized changes in tissue hydration support the existence of a circulating chloride flux. Invest Ophthalmol Vis Sci 41:3049–3055

Zampighi GA, Eskandari S, Kreman M (2000) Epithelial organization of the mammalian lens. Exp Eye Res 71:415–435